

Cell Type-specific Functions of the Lysosomal Protease Cathepsin L in the Heart^{*S}

Received for publication, April 25, 2007, and in revised form, September 21, 2007. Published, JBC Papers in Press, October 17, 2007, DOI 10.1074/jbc.M703447200

Daniel Spira[‡], Jörg Stypmann[§], Desmond J. Tobin[¶], Ivonne Petermann[‡], Christian Mayer[‡], Sascha Hagemann[‡], Olga Vasiljeva[‡], Thomas Günther^{||}, Roland Schüle^{||}, Christoph Peters[‡], and Thomas Reinheckel^{‡1}

From the [‡]Institut für Molekulare Medizin und Zellforschung, Albert-Ludwigs-Universität Freiburg, D-79104 Freiburg, Germany, [§]Medizinische Klinik und Poliklinik C (Kardiologie und Angiologie) und Zentrale Projektgruppe IVa (Kleintierdiagnostik) des Interdisziplinären Zentrums für Klinische Forschung Münster, Universitätsklinikum Münster, D-48149 Münster, Germany, [¶]Medical Biosciences, School of Life Sciences, University of Bradford, Bradford Bd7 1DP, West Yorkshire, United Kingdom, and ^{||}Universitäts-Frauenklinik und Zentrum für Klinische Forschung, Klinikum der Albert Ludwigs-Universität Freiburg, D-79106, Freiburg, Germany

Deficiency of the lysosomal cysteine protease cathepsin L (Ctsl) in mice results in a phenotype affecting multiple tissues, including thymus, epidermis, and hair follicles, and in the heart develops as a progressive dilated cardiomyopathy (DCM). To understand the role of Ctsl in the maintenance of regular heart morphology and function, it is critical to determine whether the DCM in *Ctsl*^{-/-} mice is primarily because of the lack of Ctsl expression and activity in the cardiomyocytes or is caused by the additional extracardiac pathologies. Cardiomyocyte-specific expression of Ctsl in *Ctsl*^{-/-} mice, using an α -myosin heavy chain promoter-Ctsl transgene, results in improved cardiac contraction, normal mRNA expression of atrionatriuretic peptide, normal heart weight, and regular ultrastructure of cardiomyocytes. Epithelial expression of cathepsin L2 (CTSL2) by a K14 promoter-CTSL2-transgene resulted in rescue of the *Ctsl*^{-/-} hair loss phenotype. In these mice, cardiac atrionatriuretic peptide expression and end systolic heart dimensions were also significantly attenuated. However, cardiac contraction was not improved, and increased heart weight as well as the typical changes in lysosomal ultrastructure of *Ctsl*^{-/-} hearts persisted. Myocardial fibrosis was detected in all *Ctsl*^{-/-} mice irrespective of transgene-mediated cardiac Ctsl expression or extracardiac CTSL2 expression. Expression of collagen 1 was not enhanced in *Ctsl*^{-/-} hearts, but a reduced collagenolytic activity suggests a role for Ctsl in collagen turnover by cardiac fibroblasts. We conclude that the DCM of *Ctsl*^{-/-} mice is primarily caused by absence of the protease in cardiomyocytes, whereas the complex gross phenotype of Ctsl-deficient mice, *i.e.* the fur defect, results in additional stress to the heart.

Cardiomyopathies represent a heterogeneous group of heart diseases characterized by progressive myocardial remodeling that results in impaired pump function of the heart (1). Among other etiologic factors, abnormality of lysosomes and lysosomal hydrolases have been shown to cause myocardial heart disease. Thus, cardiomyopathies have been described in hereditary deficiencies of lysosomal glycosidases, like in mucopolysaccharidoses and glycogenoses (2, 3). Deficiency of LAMP-2 (lysosome-associated membrane protein-2) has been shown to induce accumulation of autophagic vacuoles and to cause Danon disease, leading to severe myopathy of cardiac and skeletal muscles (4, 5). Furthermore, LAMP-2-deficient mice manifest a Danon disease-like vacuolar cardioskeletal myopathy (6). In hearts from cases of dilated cardiomyopathy (DCM),² increased activity of lysosomal enzymes was found (7), and autophagic degeneration was proposed to be an important mechanism (8). Among the many lysosomal protease types, “cathepsins” are expressed in the heart at considerable levels, although their specific roles in maintaining the cardiac form-function relationship have not been defined yet.

The human lysosomal cysteine cathepsins represent a family of 11 papain-like proteolytic enzymes (clan CA, family C1) with a principal subcellular localization in the endosomal/lysosomal compartment. Seven of these peptidases, the cathepsins B, C, F, H, L, O, and X/Z, exhibit ubiquitous but nevertheless differential expression in mammalian tissues. Other papain-like cysteine peptidases are known to exhibit cell type-specific expression, *e.g.* cathepsin K is mainly found in osteoclasts and cathepsin S is predominantly expressed in peripheral antigen-presenting cells (9, 10). Traditionally, lysosomal cysteine peptidases are considered to execute unspecific bulk proteolysis inside the lysosome, which supports a homeostatic function of these enzymes (11). However, there is growing evidence for specific intra- and extracellular functions of these papain-like enzymes (12, 13). For their extracellular actions, lysosomal peptidases are secreted in considerable amounts (14–16). More recently, functions of cysteine cathepsins have been identified

^{*} This work was supported by Deutsche Forschungsgemeinschaft Grants Re 1584/2-1/2-2 and Sonderforschungsbereich 656 MoBil (project C3). The costs of publication of this article were defrayed in part by the payment of page charges. This article must therefore be hereby marked “advertisement” in accordance with 18 U.S.C. Section 1734 solely to indicate this fact.

^S The on-line version of this article (available at <http://www.jbc.org>) contains supplemental Table and Figs. S1–S2.

¹ To whom correspondence should be addressed: Institut für Molekulare Medizin und Zellforschung; Stefan Meier Strasse 17, D-79104 Freiburg, Germany. Fax: 49-761-203-9634; E-mail: thomas.reinheckel@uniklinik-freiburg.de.

² The abbreviations used are: DCM, dilated cardiomyopathy; ANP, atrionatriuretic peptide; Ctsl, cathepsin L; CTSL2, cathepsin L2; α MHC, α -myosin heavy chain; PNS, postnuclear supernatants; RT, reverse transcription; Tg, transgenic.

in the cytoplasm, the nucleus, and even in the mitochondrion (17–21).

Interestingly, it was shown that 1-year-old cathepsin L (Ctsl) knock-out mice develop heart disease that resembles many features of human dilated cardiomyopathy (22). Complete deficiency of Ctsl in these mice causes interstitial fibrosis in the myocardium and pleomorphism of cardiomyocyte nuclei, histological alterations characteristic of human cardiomyopathies, as well as cardiac chamber dilation, and impaired cardiac contraction at 12 months of age. Recently it was confirmed that deficiency of Ctsl in the heart primarily affects the lysosomal system, particularly by increasing the number and changing the morphology of acidic organelles, although without the accumulation of specific lysosomal storage materials (23). Furthermore, these defects in the acidic compartments of Ctsl-deficient cardiomyocytes result in complex biochemical and cellular alterations leading to loss of cytoskeletal proteins and mitochondrial impairment, which contribute to cardiomyocyte dysfunction (23). Interestingly, the skeletal muscles of *Ctsl*^{-/-} mice are not pathologically altered. However, Ctsl-deficient mice develop spontaneous phenotypes in addition to DCM. Most prominent are periodic hair loss and epidermal thickening (24, 25). It has been shown that these phenotypes are caused by a critical role of Ctsl in endosomal/lysosomal termination of growth factor signaling in keratinocytes (26). Furthermore, Ctsl-deficient mice show a reduced number of CD4⁺-T-cells because of a reduced positive selection in the thymus and decreased volume of trabecular bones (27–29).

Because of this complex phenotype of Ctsl knock-out mice, we set out to investigate whether their cardiomyopathy is primarily caused by defective Ctsl activity in the myocardium or secondary to the other extracardiac phenotypes. Here we address this question by transgenic expression of murine Ctsl in the heart of *Ctsl*^{-/-} mice and by transgenic expression of human CTSL2 (the ortholog of mouse Ctsl) in keratin 14-expressing epithelia of *Ctsl*^{-/-} mice.

EXPERIMENTAL PROCEDURES

Generation and Maintenance of Tg(α MHC-Ctsl) Transgenics and Tg(α MHC-Ctsl);*Ctsl*^{-/-} Mice—The full-length murine Ctsl cDNA (1.1 kb), including the stop codon, was inserted into an expression cassette that included the cloning vector pBSKII SK+ (Stratagene), a murine α -myosin heavy chain promoter (provided by J. Gulick), and a transcription termination/polyadenylation fragment (poly(A), 0.63 kb) of the human growth hormone gene (30). The plasmid was injected into fertilized oocytes from FVB/n inbred mice. The oocytes were subsequently transferred into the oviducts of pseudo-pregnant recipient females. Mouse tail DNA was analyzed for integration of the transgene (founder analysis and routine genotyping) by PCR with transgene-specific primers 5'-TGTAACGGAGGCCTGATGGATTTT-3' and 5'-CCCGGTCTTTGGCTATTTTGATGT-3'. The resultant founder animals were mated with *Ctsl*^{+/-} mice (24), which are incipient transgenic (N6) for the FVB/n background. Transgene-positive and transgene-negative Ctsl knock-out (*Ctsl*^{-/-}) or wild-type (*Ctsl*^{+/+}) mice with the genotypes *Ctsl*^{+/+}, *Ctsl*^{-/-}, Tg(α MHC-Ctsl);*Ctsl*^{+/+}, and Tg(α MHC-Ctsl);*Ctsl*^{-/-} were obtained. Littermate controls

were used for all experiments. The generation, maintenance, and breeding of the mice as well as animal experiments were reviewed and performed in accordance with the German law for animal protection (Tierschutzgesetz).

Generation of Tg(K14-CTSL2);*Ctsl*^{-/-} Mice—Ctsl knock-out mice with transgenic expression of human CTSL2 (synonym cathepsin V) under the epithelial cytokeratin K14 promoter have been generated as described previously (31) and are named Tg(K14-CTSL2);*Ctsl*^{-/-} mice here. These mice are incipient congenic (N7) for the FVB/n-background.

Morphometry, Histology, and Immunohistochemistry—The body and heart weights were determined by weighing the body immediately after death and the heart after removal of both atria. The myocardium was washed in phosphate-buffered saline and fixed in 4% buffered formalin for 24 h. The fixed hearts were embedded in paraffin, and 7- μ m thick serial sections were cut, deparaffinized, and rehydrated, and extracellular matrix glucosaminoglycans were stained with Mowry staining (32). For immunohistochemistry of back skin, sections of 5- μ m thickness were deparaffinized and rehydrated. Mouse anti-human CTSL2 antibody (R & D Systems; 1:2000 dilution at 4 °C for 16 h) was used for the detection of CTSL2. Detection of the primary antibody was performed using the EnVision™ kit (Dako Cytomation) according to the manufacturer's instructions.

High Resolution Light Microscopy and Transmission Electron Microscopy—The hearts were removed and immediately fixed in half-strength Karnovsky's fixative as 3-mm³ tissue cubes. The tissues were postfixed in 2% osmium tetroxide and embedded in araldite resin. Semithin sections were stained with toluidine blue/borax, examined by light microscopy, and photographed (Leitz). Ultrathin sections were stained with uranyl acetate and lead citrate, examined, and photographed using a Jeol 1200EX transmission electron microscope (Jeol, Japan). Multiple blocks were examined from each heart, and 3-mm long and 1- μ m thick sections were examined by light microscopy from each block. These tissue blocks were further examined by transmission electron microscopy using ultrathin sections.

RNA Isolation, Reverse Transcription, and Quantitative Real Time PCR—Total RNA from myocardium was isolated using the RNeasy mini kit (Qiagen). Five micrograms of total RNA were reverse-transcribed by the SuperScript first strand synthesis system for RT-PCR (Invitrogen). PCR amplification and quantification of the reverse-transcribed cDNA was performed using the intercalating SYBR Green dye, cDNA/RNA/H₂O, Taq polymerase, and specific primers (β -actin, 5'-ACCAACTGGGACGATATGGAGAAGA-3' and 5'-TACGACCAGAGGCATACAGGGACAA-3'; Ctsl, 5'-GCACGGCTTTTCCATGGA-3' and 5'-CCACCTGCCTGAATTCCTCA-3'; ANP, 5'-CCTGGGCTTCTCCTCGTCTTG-3' and 5'-CCTCATCTTCTACCGGCATCTTCTC-3'; glyceraldehyde-3-phosphate dehydrogenase, 5'-TGCACCACCAACTGCTTAG-3' and 5'-GATGCAGGGATGATGTTC-3'; Col1a1, 5'-GCCAAGAAGACATCCCTGAAG-3' and 5'-TCATTGCATTGCACGTCATC-3') under the following conditions: 1 cycle for 15 min at 95 °C, 50 cycles (94 °C for 15s, 60 °C for 30s, and 72 °C for

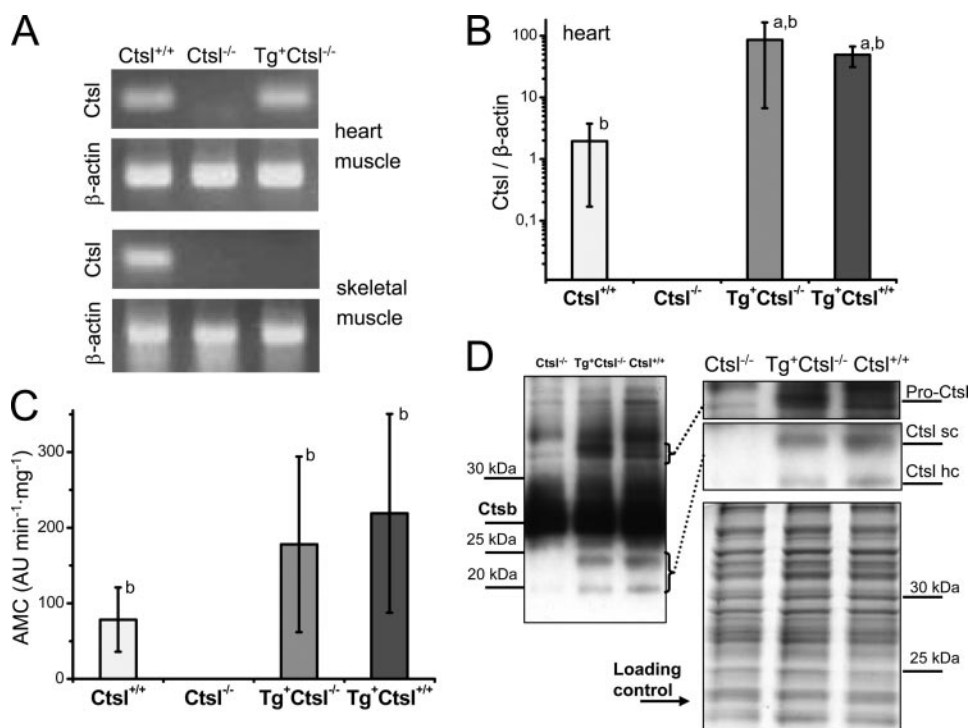


FIGURE 1. Ctsl expression in Tg(α MHC-Ctsl) mice. *A*, Ctsl expression in mRNA of heart and skeletal muscle by RT-PCR. *B*, quantification of Ctsl mRNA expression in myocardium ($n = 3-6$ per group). *C*, Ctsl activity in heart muscle by measurement of the hydrolysis of the fluorogenic dipeptide benzyloxycarbonyl-Phe-Arg-7-amido-4-methylcoumarin (AMC) in presence of the cathepsin B inhibitor CA-074 ($n = 3-5$ per group). *D*, detection of the zymogen (Pro-Ctsl) as well as the single (sc) and heavy chain (hc) forms of Ctsl by the activity-based probe DCG-04 (see Ref. 33, representative of three independent experiments). Ctsb indicates the cathepsin B band. Control, Coomassie stain for loading control. Tg⁺Ctsl^{+/+}, Tg(α MHC-Ctsl);Ctsl^{+/+}. Tg⁺Ctsl^{-/-}, Tg(α MHC-Ctsl);Ctsl^{-/-}. *a*, $p < 0.05$ versus Ctsl^{+/+}; *b*, $p < 0.05$ versus Ctsl^{-/-}.

30s) in the MyiQTM single color real time PCR detection system (Bio-Rad).

Measurement of Proteolytic Activities—Myocardial tissue was Dounce-homogenized in 150 mM NaCl, 50 mM Tris, 5 mM CaCl₂ (pH 7.6), and postnuclear supernatants (PNS) were obtained by centrifugation at 1000 × *g* for 10 min. Assay for DQ-Collagen and DQ-Gelatin (both from Invitrogen) degradation in the PNS was according to the manufacturer's protocol. Organelles were isolated by centrifuging the PNS for 20 min at 17,000 × *g* and resuspension of the organelle pellet in 100 mM sodium acetate, 1 mM EDTA, 0.05% Brij 35 (pH 5.5). Ctsl proteolytic activity was determined by hydrolysis of the fluorogenic dipeptide benzyloxycarbonyl-Phe-Arg-4-methylcoumarin-7-amide (25 μ M; Bachem) in the presence of the CTSB-specific inhibitor CA-074 (150 nM; Bachem). The release of 7-amino-4-methylcoumarin was continuously monitored for 20 min by spectrofluorometry at excitation and emission wavelengths of 370 and 460 nm, respectively.

Labeling of Cysteine Protease-active Sites with DCG-04—DCG-04 binds covalently to the active site of cysteine cathepsins and contains a biotin tag (33). 10 μ g of protein from heart organelles was incubated with DCG-04 (10 μ M; courtesy of M. Bogoy, University of California, San Francisco) for 1 h at room temperature. Subsequently, the lysates were diluted in SDS sample buffer and boiled for 10 min at 95 °C. Samples were subjected to SDS-PAGE (15% gel) and blotted on Hybond-P-polyvinylidene difluoride membrane (GE Healthcare). The

membrane was incubated with streptavidin-peroxidase complex for 2 h, and protease-bound DCG-04 was visualized by the SuperSignalTM chemiluminescent substrate (Pierce).

Echocardiography and Cardiac Doppler Examination—Echocardiographic examination was performed under inhalation anesthesia with 0.8–1.0% isoflurane. Transthoracic Doppler echocardiography was performed with a digital cardiac ultrasound machine equipped with a 15-MHz linear phased-array transducer and a 12-MHz short focal length-phased array transducer (SONOS 5500, C1 software package, Philips Medical Systems, The Netherlands). Both the parasternal long axis and short axis views were obtained. M-mode and Doppler recordings were performed at a sweep speed of 150 mm/s. Left ventricular septal and posterior wall thickness at the end of diastole as well as end diastolic and end systolic dimensions of the left ventricle were measured using leading edge to leading edge rule with the electronic caliper in M-mode (34).

The percentage of fractional shortening and ejection fraction was calculated with conversion formulas as described before (35). For determination of systolic outflow of the left ventricle and pulsed wave, Doppler signals were obtained by placing the sample volume parallel to flow during long axis view into the left ventricular outflow tract and the ascending aorta. Diastolic inflow was detected apical to the mitral valve within the left ventricle (35).

Statistics—All data are reported as arithmetic mean \pm S.D. Statistical analysis was performed by using the *U* test of Mann and Whitney. *p* values ≤ 0.05 were considered as statistically significant.

RESULTS

Cardiomyocyte-specific Expression of Ctsl in Ctsl^{-/-} Mice Using an α MHC-Ctsl Transgene—The α -myosin heavy chain promoter regulates cardiomyocyte-specific gene expression (36). Ctsl-mRNA is expressed in the heart but not in skeletal muscle of Tg(α MHC-Ctsl);Ctsl^{-/-} mice (Fig. 1A), and no Ctsl-mRNA was detected by real time PCR in liver or kidney of either Tg(α MHC-Ctsl);Ctsl^{-/-} or Ctsl^{-/-} mice (supplemental Fig. 1). Quantification of myocardial Ctsl-mRNA expression revealed more than 100-fold Ctsl-mRNA overexpression in Tg(α MHC-Ctsl);Ctsl^{-/-} and Tg(α MHC-Ctsl);Ctsl^{+/+} mice as compared with Ctsl^{+/+} controls (Fig. 1B). However, this α MHC-Ctsl transgene-induced overexpression of Ctsl-mRNA in the heart did not result in the substantial elevation of Ctsl

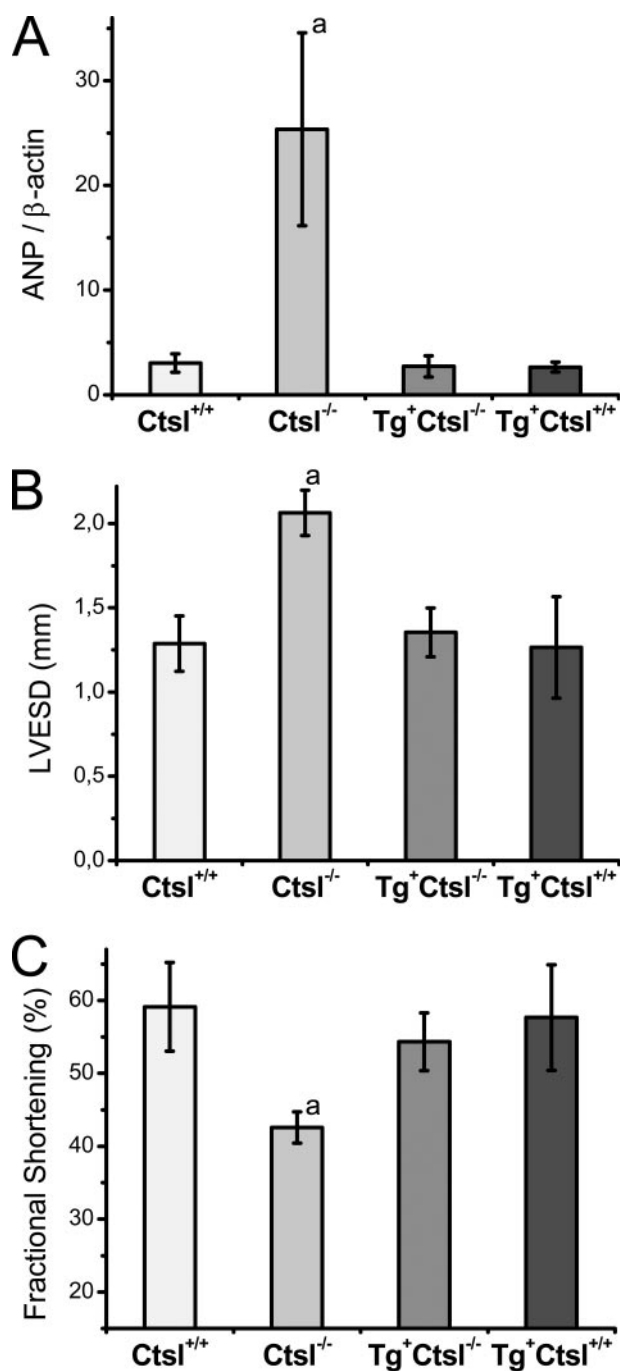


FIGURE 2. Assessment of heart function in 1-year-old $Tg(\alpha MHC-Ctsl)$ mice. A, quantification of myocardial ANP-mRNA expression by real time PCR ($n = 3-5$ per group). B, measurement of left ventricular end systolic diameters by echocardiography. C, measurement of heart contraction (Fractional Shortening) by echocardiography. $Tg^{+}Ctsl^{+/+}$, $Tg(\alpha MHC-Ctsl);Ctsl^{+/+}$. $Tg^{+}Ctsl^{-/-}$, $Tg(\alpha MHC-Ctsl);Ctsl^{-/-}$. *a*, $p < 0.05$ to all other columns.

activity. Rather, the level of Ctsl protein and its activity in the hearts of $Tg(\alpha MHC-Ctsl);Ctsl^{-/-}$ mice resembled that in wild-type mice (Fig. 1, C and D). Correspondingly, the pro-Ctsl band (with its active site labeled by DCG-04) was markedly prominent in $Tg(\alpha MHC-Ctsl);Ctsl^{-/-}$ hearts. This presumably represents a stage in Ctsl maturation between complete translation and incomplete processing (Fig. 1D). In summary, Ctsl is expressed selectively in myocardium

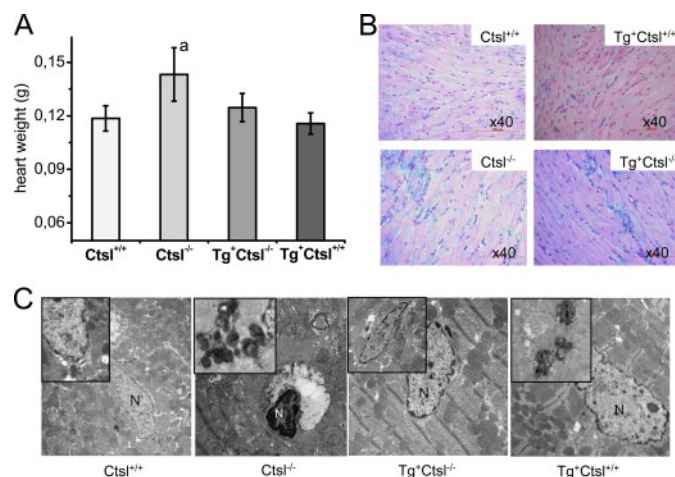


FIGURE 3. Cardiac morphology and histology of $Tg(\alpha MHC-Ctsl)$ mice. A, heart weights at 55–65 weeks ($n = 5-10$ per group). B, Mowry staining of myocardium at 40 weeks. Extracellular matrix is stained blue. C, electron microscopy of myocardium at 37 weeks. The insets highlight characteristic alterations. Figure is representative of three analyzed hearts per group. N, nucleus. $Tg^{+}Ctsl^{+/+}$, $Tg(\alpha MHC-Ctsl);Ctsl^{+/+}$. $Tg^{+}Ctsl^{-/-}$, $Tg(\alpha MHC-Ctsl);Ctsl^{-/-}$. *a*, $p < 0.05$ to all other columns.

resulting in near normal Ctsl activity levels in $Tg(\alpha MHC-Ctsl);Ctsl^{-/-}$ hearts.

Heart Function in $Tg(\alpha MHC-Ctsl);Ctsl^{-/-}$ Mice—The expression level of the ANP represents a marker for shear stress in the myocardial wall. Myocardial ANP-mRNA expression was significantly increased in $Ctsl^{-/-}$ mice versus $Ctsl^{+/+}$ controls at 55 weeks (Fig. 2A). Echocardiography revealed elevated left ventricular end systolic diameters with normal end diastolic diameters of $Ctsl^{-/-}$ hearts compared with $Ctsl^{+/+}$ controls at 55 weeks (Fig. 2B and supplemental Table), which lead to a decrease in fractional shortening indicating a systolic pump failure with reduced ventricular contraction in $Ctsl^{-/-}$ mice (Fig. 2C). Moreover, significant dilation of $Ctsl^{-/-}$ atria (supplemental Table) was noticed, matching well the clinical picture of a dilated cardiomyopathy. Cardiomyocyte-specific Ctsl expression in $Tg(\alpha MHC-Ctsl);Ctsl^{-/-}$ mice resulted in normal myocardial ANP-mRNA levels (Fig. 2A), normal end systolic, and end diastolic diameters of the left ventricle (Fig. 2B, supplemental Table) leading to improved fractional shortening (Fig. 2C). Atrial dilation was not seen in $Tg(\alpha MHC-Ctsl);Ctsl^{-/-}$ mice (supplemental Table). These results suggest a rescue of $Ctsl^{-/-}$ heart function by cardiomyocyte-specific expression of Ctsl ($Tg(\alpha MHC-Ctsl);Ctsl^{-/-}$ mouse).

Heart Morphology and Histology of $Tg(\alpha MHC-Ctsl);Ctsl^{-/-}$ Mice—Heart weights were significantly increased in $Ctsl^{-/-}$ versus $Ctsl^{+/+}$ mice. Cardiomyocyte-specific Ctsl expression in $Tg(\alpha MHC-Ctsl);Ctsl^{-/-}$ mice normalized the heart weight to wild-type levels (Fig. 3A). However, hearts of both $Ctsl^{-/-}$ and $Tg(\alpha MHC-Ctsl);Ctsl^{-/-}$ mice showed more prominent staining of extracellular matrix when compared with $Ctsl^{+/+}$ hearts, indicating the presence of interstitial fibrosis. No fibrosis was observed in hearts of $Tg(\alpha MHC-Ctsl);Ctsl^{+/+}$ mice showing that the expression of the $\alpha MHC-Ctsl$ transgene does not, in itself, cause interstitial fibrosis (Fig. 3B). Investigation of myocardial ultrastructure in $Ctsl^{+/+}$ hearts revealed regular muscle fiber morphology with normal mitochondria and only few,

TABLE 1

Synopsis of heart phenotypes in cathepsin L mutant mice

Ctsl^{-/-} indicates Ctsl "knock-out"; Tg(α MHC-Ctsl);*Ctsl*^{-/-} indicates Ctsl "knock-out" with additional α MHC-Ctsl transgene; Tg(K14-CTSL2);*Ctsl*^{-/-} indicates Ctsl "knock-out" with additional K14-CTSL2 transgenes.

Genotypes	Heart function		Heart morphology		
	Molecular markers	Echocardiography	Heart weight	Fibrosis	Myocardial ultrastructure
<i>Ctsl</i> ^{-/-}	Pathological	Pathological	Pathological	Pathological	Pathological
Tg(α MHC-Ctsl); <i>Ctsl</i> ^{-/-}	Normal	Normal	Normal	Pathological	Normal
Tg(K14-CTSL2); <i>Ctsl</i> ^{-/-}	Pathological but partially normalized as compared with <i>Ctsl</i> ^{-/-}	Pathological but partially normalized as compared with <i>Ctsl</i> ^{-/-}	Pathological	Pathological	Pathological

small, electron-dense lysosomes (Fig. 3C). This normal morphology was also detected in the hearts of Tg(α MHC-Ctsl); *Ctsl*^{+/+} mice. Furthermore, electron microscopy revealed nuclear degeneration (Fig. 3C), considerable lysosomal accumulation (Fig. 3C and Fig. 5C), and mitochondrial degeneration with vacuolization (Fig. 5C) in cardiomyocytes of *Ctsl*^{-/-} mice aged 37 or 60 weeks. As cellular vacuolization and signs of lysosomal accumulation were considerably more predominant in *Ctsl*^{-/-} hearts at 60 weeks compared with 37 weeks of age (data not shown), age-associated progression of cardiomyopathy seems conceivable. Tg(α MHC-Ctsl);*Ctsl*^{-/-} heart ultrastructure showed similar morphology as age-matched *Ctsl*^{+/+} control hearts. No nuclear dysmorphism or degeneration and only occasional vacuolization of cardiomyocytes were observed (Fig. 3C). Thus, the characteristic changes of the *Ctsl*^{-/-} cardiac ultrastructure were prevented by the expression of the α MHC-Ctsl-transgene. In summary, heart weight and cardiomyocyte ultrastructure is rescued by cardiomyocyte-specific expression of Ctsl in Tg(α MHC-Ctsl);*Ctsl*^{-/-} mice, whereas myocardial fibrosis persists (Table 1).

Extracardiac Expression of Human CTSL2 in Tg(K14-CTSL2);*Ctsl*^{-/-} Mice—*Ctsl*^{-/-} mice show a phenotype of periodic hair loss (24–26). Thus, the cardiomyopathy of *Ctsl*^{-/-} mice might be aggravated by the metabolic stress associated with heat loss. *Ctsl*^{-/-} mice with transgenic expression of human CTSL2 under the epithelial K14 promoter (Tg(K14-CTSL2);*Ctsl*^{-/-} mice) show normalization of hair and skin phenotype (31). We investigated whether the characteristic cardiac changes of Ctsl-deficient mice persist in Tg(K14-CTSL2);*Ctsl*^{-/-} mice with normal hair growth. Human CTSL2-mRNA was expressed in the skin but not in the heart of Tg(K14-CTSL2);*Ctsl*^{-/-} mice (supplemental Fig. 2A). CTSL2 expression at the protein level was detected in the epidermis and hair follicle of Tg(K14-CTSL2);*Ctsl*^{-/-} but not in *Ctsl*^{+/+} mice (supplemental Fig. 2B).

Heart Function of Tg(K14-CTSL2);*Ctsl*^{-/-} Mice—Compared with *Ctsl*^{-/-} mice the extracardiac CTSL2 expression in Tg(K14-CTSL2);*Ctsl*^{-/-} mice resulted in reduced myocardial ANP-mRNA levels (Fig. 4A), and reduced end systolic and end diastolic diameters of the left ventricle (Fig. 4B, supplemental Table). However, heart function as assessed by cardiac contraction (fractional shortening) and ejection fractions remained pathologically impaired, whereas atrial dilation was not seen in Tg(K14-CTSL2);*Ctsl*^{-/-} mice (Fig. 4C; supplemental Table). As fractional shortening and ejection fraction are the most important features in heart contraction by echocardiography, we conclude that there was merely incomplete improvement of *Ctsl*^{-/-} heart function by extracardiac expression of CTSL2

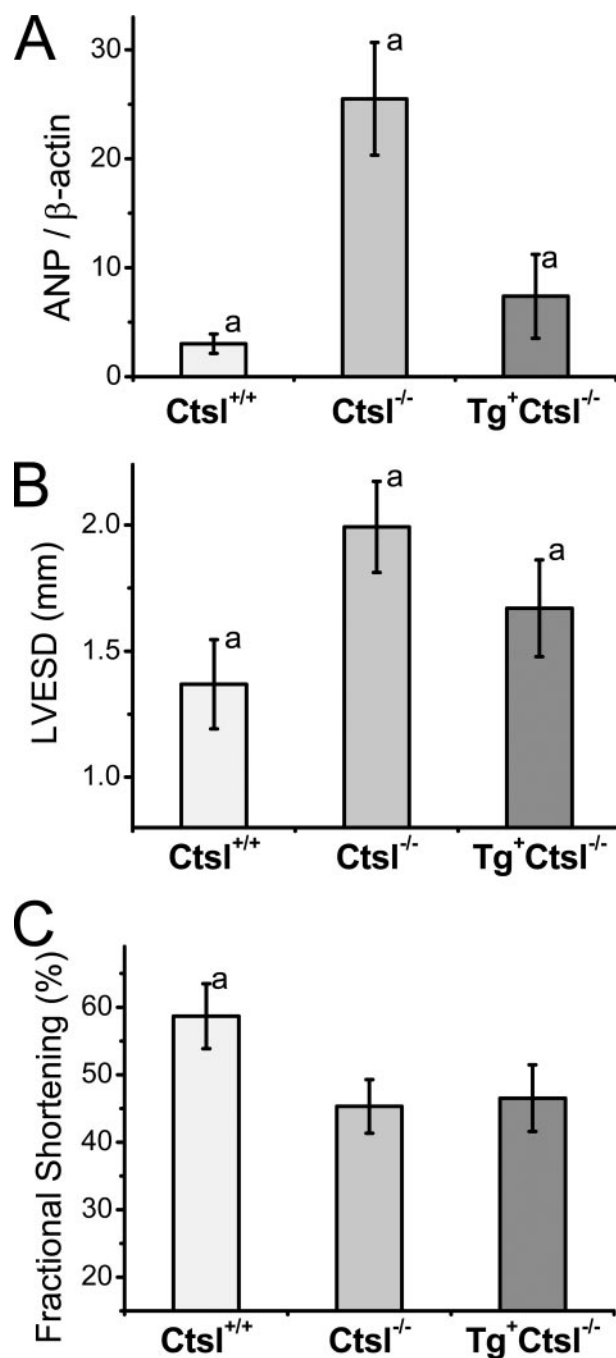


FIGURE 4. Assessment of heart function in Tg(K14-CTSL2);*Ctsl*^{-/-} mice. A, transcription of ANP-mRNA expression by quantitative RT-PCR with ANP-versus β -actin-specific primers ($n = 3-5$ per group). B, measurement of left ventricular end systolic diameters; C, heart contraction (Fractional Shortening) by echocardiography. Tg⁺*Ctsl*^{+/+}, Tg(K14-CTSL2);*Ctsl*^{+/+}. Tg⁺*Ctsl*^{-/-}, Tg(K14-CTSL2);*Ctsl*^{-/-}. a, $p < 0.05$ to all other columns.

DCM in Cathepsin L Knock-out Mice

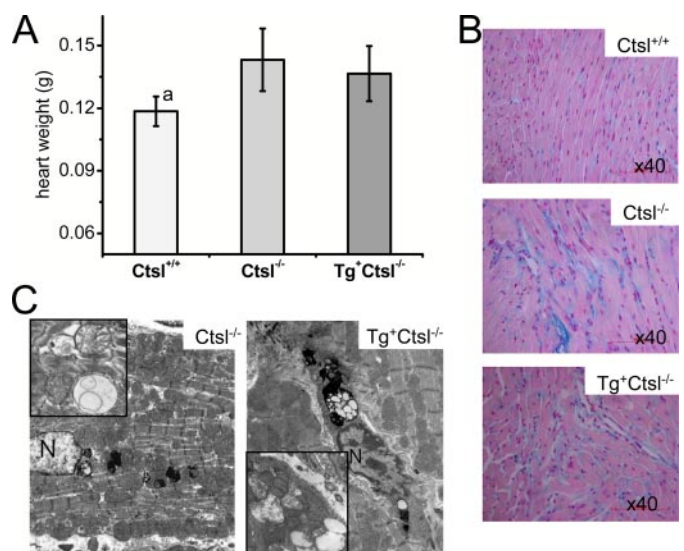


FIGURE 5. Cardiac morphology and histology of the Tg(K14-CTSL2); *Ctsl*^{-/-} mouse. *A*, heart weights at 55–65 weeks ($n = 7$ –11 per group). *B*, Mowry staining of myocardium at 65 weeks. Extracellular matrix is stained blue ($n = 3$ per group). *C*, electron microscopy of myocardium at 60 weeks. The insets highlight corresponding characteristic alterations. *N*, nucleus. $Tg^{+}Ctsl^{+/+}$, Tg(K14-CTSL2); $Ctsl^{+/+}$. $Tg^{+}Ctsl^{-/-}$, Tg(K14-CTSL2); $Ctsl^{-/-}$. $a, p < 0.05$ to all other columns.

(Tg(K14-CTSL2); $Ctsl^{-/-}$ mouse) with normalization of hair and skin phenotypes.

Pathologic Heart Morphology and Histology in Tg(K14-CTSL2);*Ctsl*^{-/-} Mice—Heart weights of Tg(K14-CTSL2); $Ctsl^{-/-}$ were similarly increased as those of age-matched $Ctsl^{-/-}$ mice (Fig. 5*A*). Hearts of $Ctsl^{-/-}$ and Tg(K14-CTSL2); $Ctsl^{-/-}$ mice showed more prominent staining of extracellular matrix when compared with age-matched $Ctsl^{+/+}$ hearts, indicating an interstitial fibrosis (Fig. 5*B*). Ultrastructural analysis of Tg(K14-CTSL2); $Ctsl^{-/-}$ myocardium revealed considerable lysosomal accumulation and mitochondrial degeneration with significant vacuolization (Fig. 5*C*). These ultrastructural changes are similar to those seen in age-matched $Ctsl^{-/-}$ hearts (Fig. 5*C*). These results indicate a persistent myocardial fibrosis and pathologic cardiac ultrastructure regardless of the normalization of the hair phenotype and body weight in Tg(K14-CTSL2); $Ctsl^{-/-}$ mice.

Interstitial Fibrosis—Interestingly, interstitial fibrosis was not markedly improved by cardiac or extracardiac expression of Ctsl. However, the transcription of collagen I, which represents the major fibrotic collagen in the myocardium, was not increased in $Ctsl^{-/-}$ hearts (Fig. 6*A*). Thus to address this, we decided to measure gelatinolytic and collagenolytic activities in the myocardial homogenates by degradation of fluorescence-quenched DQ-gelatin and DQ-collagen to assess whether fibrosis could be caused by impaired turnover of extracellular matrix proteins (Fig. 6*B*). When compared with wild-type mice, the proteolytic cleavage of both substrates was significantly reduced in $Ctsl^{-/-}$ hearts and in hearts of Tg(K14-CTSL2); $Ctsl^{-/-}$ mice. Interestingly, transgenic re-expression of Ctsl in cardiomyocytes normalized the cleavage of DQ-gelatin, but degradation of DQ-collagen remained at the level of $Ctsl^{-/-}$ hearts. Thus, the fibrosis observed in $Ctsl$ -deficient hearts might be caused by defects of collagen turnover in cardiac fibroblasts.

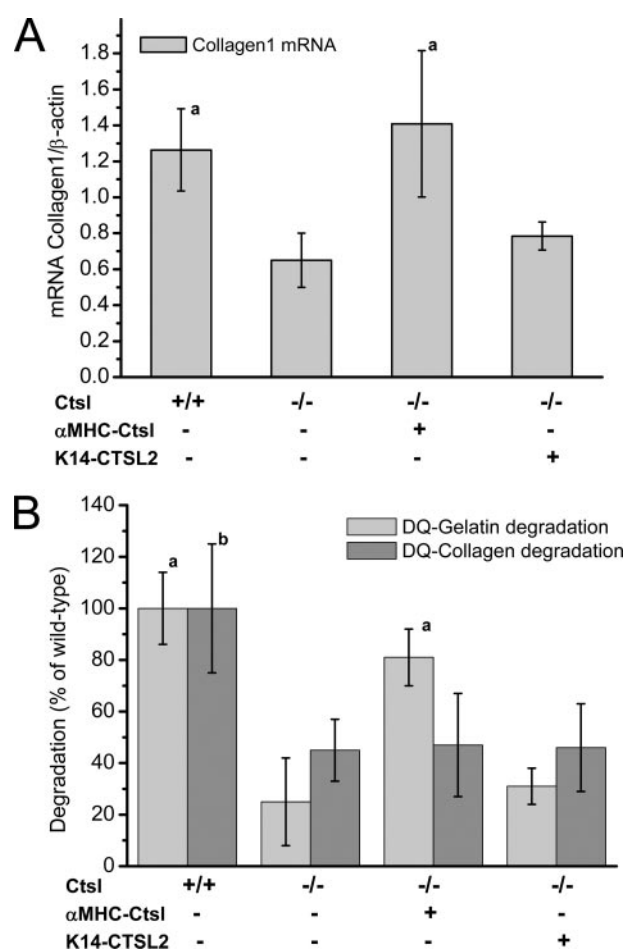


FIGURE 6. Quantification of cardiac type I collagen mRNA and measurement of cardiac gelatinolytic and collagenolytic activities. *A*, transcription of collagen type I mRNA from left ventricular myocardium by quantitative RT-PCR (age 55–65 weeks, $n = 3$ –5 per group). *B*, gelatinolytic and collagenolytic activity in myocardial homogenates was measured by degradation of fluorescent-labeled DQ-gelatin and DQ-collagen (age 50–55 weeks, $n = 4$ per group). $a, p < 0.05$ compared with $Ctsl^{-/-}$ (2nd column) and Tg(K14-CTSL2); $Ctsl^{-/-}$ (4th column); $b, p < 0.05$ compared with all other columns.

DISCUSSION

Ctsl is known as a highly potent endoprotease of the cysteine cathepsin family. It is ubiquitously expressed; however, Ctsl expression levels vary considerably among different cell types. Furthermore, Ctsl executes critical functions in specific cell and tissue types as has been revealed by analysis of $Ctsl$ -deficient mouse models (12, 24, 37). In addition to the cardiomyopathy addressed here (22, 23), a delayed and reduced tumor development in the Rip1-Tag2 model for pancreatic islet cell carcinomas has been detected in $Ctsl$ -deficient mice (38). Ctsl contributes to maturation and release of enkephalin and thyroid hormone (39, 40). Important cell type-specific functions of Ctsl include antigen presentation and maturation of major histocompatibility class II complexes in thymic cortex epithelial cells (27, 41), and periodic hair loss as well as epidermal hyperproliferation and thickening (24, 25). The most convincing evidence for cell autonomous functions of Ctsl has been provided by the rescue of the immune and skin phenotypes by transgenic mice with specific re-expression of Ctsl in thymic cortex epithelial cells and keratinocytes, respectively (26, 31).

Here we determined whether the cardiomyopathy in *Ctsl*-deficient is primarily caused by the cathepsin defect in cardiomyocytes is secondary to the other phenotypes. Cardiomyocyte-specific expression of murine *Ctsl* by the α MHC promoter in *Ctsl*^{-/-} mice results in improvements of all parameters of heart ultrastructure and heart function with the notable exception of myocardial fibrosis (Table 1). Expression of CTSL2 (the human ortholog of *Ctsl* with about 75% amino acid identity) under control of the human cytokeratin 14 (K14) promoter in *Ctsl*^{-/-} mice rescues the skin phenotype (*i.e.* periodic hair loss and epidermal thickening) and normalizes of CD4-T-cell counts (31). Here we show that the K14-CTSL2 transgene is not expressed in the heart. Interestingly, K14-CTSL2 expression also results in a significant improvement of left ventricular end systolic diameters in *Ctsl*^{-/-} mice. In support of the more favorable heart dimensions is the significantly reduced mRNA expression of ANP, a marker for sheer stress in the myocardial wall (42–44). However, myocardial contraction/fractional shortening and ultrastructure are not normalized in the Tg(K14-CTSL2);*Ctsl*^{-/-} mice. Thus, metabolic stress exerted by heat loss because of the hair loss phenotype of *Ctsl*^{-/-} mice may support cardiomyopathy development but is apparently not causing the initiation of cardiac pathogenesis. We have previously reported an impairment of cardiomyocyte ultrastructure in *Ctsl*^{-/-} hearts in newborn mice as the earliest detectable pathogenic event in development of cardiomyopathy in *Ctsl*-deficient mice (23). Specifically an increased number and size of “acidic” vesicles of the endosomal/lysosomal compartment has been observed. Similar observations have been made in keratinocytes, which are the critical cells for the *Ctsl*^{-/-} skin phenotype (25, 26). This suggests an alteration of the endosomal/lysosomal compartment by *Ctsl* deficiency as a common cause of the prominent skin and heart phenotypes of *Ctsl*-deficient mice. In the case of *Ctsl*^{-/-} keratinocytes it has been shown that an imbalance of degradation and recycling of growth factors (*e.g.*, epidermal growth factor) causes a sustained mitogenic signaling and, hence, hyperproliferation in the epidermis and hair follicles of affected mice (25, 26). Extensive proteome comparison of *Ctsl*-deficient and wild-type hearts revealed decreased levels of the sarcomere-associated proteins α -tropomyosin, desmin, and calsarcin 1, as well as changes in levels of metabolic enzymes and components of the vesicular transport system (23). Bioinformatics pathway analysis suggested a switch to anaerobic catabolism and the impairment of mitochondrial respiration. This interpretation was supported by a 50% reduction in resting state oxygen consumption and impaired respiration capacity in *Ctsl*^{-/-} myocardial homogenates (23). Thus, *Ctsl* deficiency in hearts results in metabolic and sarcomeric alterations that promote DCM development.

Strikingly the *Ctsl*^{-/-}-associated interstitial fibrosis is not rescued when expression of *Ctsl* activity is returned to cardiomyocytes (by the α MHC-*Ctsl* transgene) or to keratinocytes and thymic cortex epithelium (by the K14-CTSL2 transgene). Thus, fibrosis appears to be independent of the specific *Ctsl* functions in cardiomyocytes, epidermis, hair follicles, and the immune system. Fibrosis is an important pathologic hallmark of cardiomyopathies resulting in conduction alterations and cardiac valve defects (1, 45, 46). Both arrhythmias and valve insufficien-

cies have been detected in *Ctsl*^{-/-} hearts (22). Because we show that collagen 1 expression is not enhanced in *Ctsl*-deficient myocardium, it is most likely that accumulation of collagen in the extracellular matrix is because of a defective collagen turnover. Although *Ctsl* is mainly located in the endosomal/lysosomal compartment, about 10% of the zymogen is physiologically secreted, can be extracellularly activated, and has been reported to process extracellular matrix proteins such as fibronectin, laminin, and type I, IV, and XVIII collagen (47–49). Supporting this hypothesis is the marked decrease in collagenolytic and gelatinolytic activities in the affected myocardium (Fig. 6B). Interestingly, transgenic re-expression of *Ctsl* in cardiomyocytes normalized the cleavage of DQ-gelatin, but degradation of DQ-collagen remained at the level of *Ctsl*^{-/-} hearts (Fig. 6B). We interpret this finding to mean that DQ-gelatin, which presents a highly denatured collagen preparation, is readily cleaved by a number of potent endoproteases, with *Ctsl* being a major representative. In contrast, DQ-collagen is a more complex native collagen preparation requiring the action of specific collagenases. Based on our present genetic studies, these collagenases are likely to be activated either directly or indirectly (*i.e.* by inhibitor degradation) by *Ctsl* derived from the cardiac fibroblasts. These *in vivo* results are in line with the recent observation that calvarial bone osteoclasts do not use matrix metalloproteinases for bone matrix resorption in the absence of *Ctsl* (29).

In summary, *Ctsl* exerts multiple cell type-specific functions in the heart. Its deficiency causes structural and functional alterations within cardiomyocytes and affects the collagen turnover of cardiac fibroblasts. In addition, the complex gross phenotype of *Ctsl*-deficient mice, *i.e.* the fur defect, results in additional stress for the heart. Taken together, pathogenic cardiac remodeling is initiated that leads to manifest cardiac dysfunction in 1-year-old mice.

Acknowledgments—We thank Susanne Dollwet-Mack and Nicole Klemm (Institut für Molekulare Medizin und Zellforschung, Freiburg) for excellent technical assistance. We thank J. Gulick (Children's Hospital Medical Center, University of Cincinnati) for the plasmid containing the α MHC promoter and M. Bogoy (Dept. of Pathology, Stanford University) for supply of DCG-04.

REFERENCES

- Towbin, J. A., and Bowles, N. E. (2002) *Nature* **415**, 227–233
- Guertl, B., Noehammer, C., and Hoefler, G. (2000) *Int. J. Exp. Pathol.* **81**, 349–372
- Strauch, O. F., Stypmann, J., Reinheckel, T., Martinez, E., Haverkamp, W., and Peters, C. (2003) *Pediatr. Res.* **54**, 701–708
- Nishino, I., Fu, J., Tanji, K., Yamada, T., Shimajo, S., Koori, T., Mora, M., Riggs, J. E., Oh, S. J., Koga, Y., Sue, C. M., Yamamoto, A., Murakami, N., Shanske, S., Byrne, E., Bonilla, E., Nonaka, I., DiMauro, S., and Hirano, M. (2000) *Nature* **406**, 906–910
- Stypmann, J., Janssen, P. M., Prestle, J., Engelen, M. A., Kogler, H., Lullmann-Rauch, R., Eckardt, L., von Figura, K., Landgrebe, J., Mleczo, A., and Saftig, P. (2006) *Basic Res. Cardiol.* **101**, 281–291
- Tanaka, Y., Guhde, G., Suter, A., Eskelinen, E. L., Hartmann, D., Lullmann-Rauch, R., Janssen, P. M., Blanz, J., von Figura, K., and Saftig, P. (2000) *Nature* **406**, 902–906
- Figulla, H. R., Bardosi, A., Dechant, K., and Kreuzer, H. (1991) *Cardiology* **78**, 282–290

8. Shimomura, H., Terasaki, F., Hayashi, T., Kitaura, Y., Isomura, T., and Suma, H. (2001) *Jpn. Circ. J.* **65**, 965–968
9. Rawlings, N. D., Morton, F. R., and Barrett, A. J. (2006) *Nucleic Acids Res.* **34**, D270–D272
10. Turk, B., Turk, D., and Turk, V. (2000) *Biochim. Biophys. Acta* **1477**, 98–111
11. Barrett, A. J. (1992) *Ann. N. Y. Acad. Sci.* **674**, 1–15
12. Reinheckel, T., Deussing, J., Roth, W., and Peters, C. (2001) *Biol. Chem.* **382**, 735–741
13. Turk, V., Turk, B., and Turk, D. (2001) *EMBO J.* **20**, 4629–4633
14. Linke, M., Jordans, S., Mach, L., Herzog, V., and Brix, K. (2002) *Biol. Chem.* **383**, 773–784
15. Frosch, B. A., Berquin, I., Emmert-Buck, M. R., Moin, K., and Sloane, B. F. (1999) *APMIS* **107**, 28–37
16. Mohamed, M. M., and Sloane, B. F. (2006) *Nat. Rev. Cancer* **6**, 764–775
17. Cirman, T., Oresic, K., Mazovec, G. D., Turk, V., Reed, J. C., Myers, R. M., Salvesen, G. S., and Turk, B. (2004) *J. Biol. Chem.* **279**, 3578–3587
18. Guicciardi, M. E., Deussing, J., Miyoshi, H., Bronk, S. F., Svingen, P. A., Peters, C., Kaufmann, S. H., and Gores, G. J. (2000) *J. Clin. Investig.* **106**, 1127–1137
19. Goulet, B., Baruch, A., Moon, N. S., Poirier, M., Sansregret, L. L., Erickson, A., Bogyo, M., and Nepveu, A. (2004) *Mol. Cell* **14**, 207–219
20. Bestvater, F., Dallner, C., and Spiess, E. (2005) *BMC Cell Biol.* **6**, 16
21. Muntener, K., Zwicky, R., Csucs, G., Rohrer, J., and Baici, A. (2004) *J. Biol. Chem.* **279**, 41012–41017
22. Stypmann, J., Glaser, K., Roth, W., Tobin, D. J., Petermann, I., Matthias, R., Monnig, G., Haverkamp, W., Breithardt, G., Schmahl, W., Peters, C., and Reinheckel, T. (2002) *Proc. Natl. Acad. Sci. U. S. A.* **99**, 6234–6239
23. Petermann, I., Mayer, C., Stypmann, J., Biniowski, M. L., Tobin, D. J., Engelen, M. A., Dandekar, T., Grune, T., Schild, L., Peters, C., and Reinheckel, T. (2006) *FASEB J.* **20**, 1266–1268
24. Roth, W., Deussing, J., Botchkarev, V. A., Pauly-Evers, M., Saftig, P., Hafner, A., Schmidt, P., Schmahl, W., Scherer, J., Anton-Lamprecht, I., Von Figura, K., Paus, R., and Peters, C. (2000) *FASEB J.* **14**, 2075–2086
25. Tobin, D. J., Foitzik, K., Reinheckel, T., Mecklenburg, L., Botchkarev, V. A., Peters, C., and Paus, R. (2002) *Am. J. Pathol.* **160**, 1807–1821
26. Reinheckel, T., Hagemann, S., Dollwet-Mack, S., Martinez, E., Lohmuller, T., Zlatkovic, G., Tobin, D. J., Maas-Szabowski, N., and Peters, C. (2005) *J. Cell Sci.* **118**, 3387–3395
27. Nakagawa, T., Roth, W., Wong, P., Nelson, A., Farr, A., Deussing, J., Viladangos, J. A., Ploegh, H., Peters, C., and Rudensky, A. Y. (1998) *Science* **280**, 450–453
28. Potts, W., Bowyer, J., Jones, H., Tucker, D., Freemont, A. J., Millest, A., Martin, C., Vernon, W., Neerunjun, D., Slynn, G., Harper, F., and Maciewicz, R. (2004) *Int. J. Exp. Pathol.* **85**, 85–96
29. Everts, V., Korper, W., Hoeben, K. A., Jansen, I. D., Bromme, D., Cleutjens, K. B., Heeneman, S., Peters, C., Reinheckel, T., Saftig, P., and Beertsen, W. (2006) *J. Bone Miner. Res.* **21**, 1399–1408
30. Gulick, J., Subramaniam, A., Neumann, J., and Robbins, J. (1991) *J. Biol. Chem.* **266**, 9180–9185
31. Hagemann, S., Gunther, T., Dennemarker, J., Lohmuller, T., Bromme, D., Schule, R., Peters, C., and Reinheckel, T. (2004) *Eur. J. Cell Biol.* **83**, 775–780
32. Mowry, R. W. (1958) *Lab. Investig.* **7**, 566–576
33. Greenbaum, D., Medzihradzky, K. F., Burlingame, A., and Bogyo, M. (2000) *Chem. Biol.* **7**, 569–581
34. Sahn, D. J., DeMaria, A., Kisslo, J., and Weyman, A. (1978) *Circulation* **58**, 1072–1083
35. Stypmann, J., Engelen, M. A., Epping, C., van Rijen, H. V., Milberg, P., Bruch, C., Breithardt, G., Tiemann, K., and Eckardt, L. (2006) *Int. J. Cardiovasc. Imaging* **22**, 353–362
36. Aikawa, R., Huggins, G. S., and Snyder, R. O. (2002) *J. Biol. Chem.* **277**, 18979–18985
37. Benavides, F., Starost, M. F., Flores, M., Gimenez-Conti, I. B., Guenet, J. L., and Conti, C. J. (2002) *Am. J. Pathol.* **161**, 693–703
38. Gocheva, V., Zeng, W., Ke, D., Klimstra, D., Reinheckel, T., Peters, C., Hanahan, D., and Joyce, J. A. (2006) *Genes Dev.* **20**, 543–556
39. Yasothornsrikul, S., Greenbaum, D., Medzihradzky, K. F., Toneff, T., Bunday, R., Miller, R., Schilling, B., Petermann, I., Dehnert, J., Logvinova, A., Goldsmith, P., Neveu, J. M., Lane, W. S., Gibson, B., Reinheckel, T., Peters, C., Bogyo, M., and Hook, V. (2003) *Proc. Natl. Acad. Sci. U. S. A.* **100**, 9590–9595
40. Friedrichs, B., Tepel, C., Reinheckel, T., Deussing, J., von Figura, K., Herzog, V., Peters, C., Saftig, P., and Brix, K. (2003) *J. Clin. Investig.* **111**, 1733–1745
41. Honey, K., Nakagawa, T., Peters, C., and Rudensky, A. (2002) *J. Exp. Med.* **195**, 1349–1358
42. Loennechen, J. P., Stoylen, A., Beisvag, V., Wisloff, U., and Ellingsen, O. (2001) *Am. J. Physiol.* **280**, H2902–H2910
43. Langenickel, T., Pagel, I., Hohnel, K., Dietz, R., and Willenbrock, R. (2000) *Am. J. Physiol.* **278**, H1500–H1506
44. Yoshimura, M., Yasue, H., Okumura, K., Ogawa, H., Jougasaki, M., Mukoyama, M., Nakao, K., and Imura, H. (1993) *Circulation* **87**, 464–469
45. Hughes, S. E., and McKenna, W. J. (2005) *Heart* **91**, 257–264
46. Hughes, S. E. (2004) *Histopathology* **44**, 412–427
47. Felbor, U., Dreier, L., Bryant, R. A., Ploegh, H. L., Olsen, B. R., and Mothes, W. (2000) *EMBO J.* **19**, 1187–1194
48. Urbich, C., Heeschen, C., Aicher, A., Sasaki, K., Bruhl, T., Farhadi, M. R., Vajkoczy, P., Hofmann, W. K., Peters, C., Pennacchio, L. A., Abolmaali, N. D., Chavakis, E., Reinheckel, T., Zeiher, A. M., and Dimmeler, S. (2005) *Nat. Med.* **11**, 206–213
49. Maciewicz, R. A., and Etherington, D. J. (1988) *Biochem. J.* **256**, 433–440